NEW IMPROVED ALGORITHM FOR SKY CALIBRATION OF L-BAND RADIOMETERS JÜLBARA AND ELBARA II

M. Dimitrov[(1)], K.G. Kostov[(2)], F. Jonard[(1)], K.Z. Jadoon[(1,3)], M. Schwank[(4)], L. Weihermüller[(1)], N. Hermes[(1)], J. Vanderborght[(1)], and H. Vereecken[(1)]

[(1)]Research Centre Jülich, Institute of Bio- and Geosciences: Agrosphere (IBG 3), 52425 Jülich, GERMANY
[(2)]Bulgarian Academy of Sciences, Institute of Electronics, 1784 Sofia, BULGARIA
[(3)]Water Desalination and Reuse Center, KAUST, Thuwal, 23955-6900, SAUDI ARABIA
[(4)]German Research Centre for Geosciences, 14473 Potsdam, GERMANY

Abstract— **We propose a new algorithm for sky calibration of the L-band radiometers JÜLBARA and ELBARA II, introducing the effective transmissivities of the instruments. The suggested approach was tested using experimental data obtained at the Selhausen test site, Germany. It was shown that for JÜLBARA the effective transmissivities depend strongly on the air temperature and decrease with increasing air temperature, while for ELBARA II such strong dependence was not observed. It was also shown that the effective transmissivities account for the antenna and feed cable loss effects, and for the variations of the radiometer gain due to air temperature changes. The new calibration algorithm reduces significantly the bias of brightness temperature estimates for both radiometers, especially for JÜLBARA.**

Keywords- Calibration; microwave radiometer; sky emission

I. INTRODUCTION

The sky emission is widely used as a well known noise source for external calibration of microwave radiometers. For L-band radiometers with built-in noise sources for internal calibration of the radiometer receiver, the sky calibration is also important for periodic external calibration of the radiometer system including the antenna and the feed cables.

The main goals of this paper are: (a) to describe the new algorithm for sky calibration of the L-band radiometers JÜLBARA and ELBARA II, both of which have built-in noise sources for internal calibration (b) to present the experimental results, and (c) to compare the algorithms performance.

II. CALIBRATION ALGORITHMS

A. Internal calibration

The noise temperatures $T_{B,INT,p}$ at the radiometer inputs for horizontal and vertical polarizations were calculated as follows:

$$T_{B,INT,p} = \frac{T_{HOT} - T_{COLD}}{U_{HOT} - U_{COLD}}\left(U_p - U_{COLD}\right) + T_{COLD}, \quad (1)$$

where T_{HOT} and T_{COLD} are the noise temperatures of the internal hot and cold calibration sources ($T_{HOT} > T_{COLD}$), U_{HOT} and U_{COLD} are the corresponding instrumental raw data in units of volts at the output of the RF path, and U_p are the voltages, associated with the antenna measurements with $p = H$ and $p = V$ for horizontal (H-pol) and vertical (V-pol) polarizations, respectively. $S = (T_{HOT} - T_{COLD})/(U_{HOT} - U_{COLD})$, (K/V) is the slope of the internal calibration equation and $G = 1/S$, (V/K) is the net gain of the radiometer system including the RF-path.

B. External calibration

The radiometer systems were directed toward the sky and the brightness temperatures $T_{B,EXT,p}$ were estimated as presented below using two different algorithms.

1) Algorithm 1: Cable loss correction

As shown in [2] and [3], the noise contributions due to feed cable loss $L_{FC,p}$ (dB) and cable temperature $T_{FC,p}$ (K) can be corrected using (2)

$$T_{B,EXT,p} = \frac{T_{B,INT,p} - (1 - t_{FC,p})T_{FC,p}}{t_{FC,p}}, \quad (2)$$

where $t_{FC,p}$ is the feed cable transmissivity, which is calculated from the measured cable loss as follows:

$$t_{FC,p} = 10^{(-L_{FC,p}/10)}. \quad (3)$$

The measured air temperature was used as approximation for the cable temperature $T_{FC,p}$ as recommended in [2] and [3].

2) Algorithm 2: Effective transmissivity

We introduce an effective transmissivity $t_{eff,p}$ defined as:

$$t_{eff,p} = \frac{T_{air} - T_{B,INT,p}}{T_{air} - T_{B,MODEL}}, \quad (4)$$

where T_{air} (K) is the air temperature and $T_{B,MODEL}$ is the sky brightness temperature calculated from the model given in [4].

The new calibration algorithm is

$$T_{B,EXT,p} = \frac{T_{B,INT,p} - (1 - t_{eff,p})T_{air}}{t_{eff,p}}. \quad (5)$$

III. SKY MEASUREMENTS

The experiments were conducted at the Selhausen test site of the Research Centre Jülich (FZJ), Germany. Radiometric measurements of the sky scene were performed with L-band radiometer JÜLBARA from April till September 2011, three times a day, namely from 7 to 8 am, from 3 to 4 pm, and from 11 pm to 0 am. The ELBARA II radiometer was also oriented toward the sky and measured continuously between 11 July and 11 August 2011. Measurements of the air temperature near to the radiometer systems were carried out simultaneously with the radiometric measurements. Measurements of the feed cables physical temperatures of JÜLBARA were also collected. The radiometers were mounted on different platforms, about 30 meters from each other. For the sky measurements the radiometers were oriented toward the south and toward the north, respectively with incidence angles of 135° for JÜLBARA and 140° for ELBARA II relative to nadir.

The Dicke-type radiometer JÜLBARA was built based on the same concept as the ELBARA radiometer [1] and measures in the protected region of L-band at two frequency ranges 1.400–1.414 GHz (Channel 1 (CH1)) and 1.414–1.427 GHz (Channel 2 (CH2)), respectively. The radiometer was equipped with two internal calibration sources, namely hot noise source (338 K) and cold source (278 K), and a conical horn antenna with 12° full beamwidth at -3 dB. Detailed description of ELBARA II is given in [2]. A resistive noise source and an active cold source were used as hot and cold calibration sources, respectively, in the ELBARA II calibration assembly [2]. ELBARA II was equipped with a conical horn antenna with -3 dB full beamwidth of 24°. Both L-band radiometers worked with 10 seconds integration time. The radiometer resolution (sensitivity) was 0.1 K. One measurement cycle lasts about 45 seconds and was performed every minute [2].

IV. RESULTS AND DISCUSSION

Equation (1) was used to calculate $T_{B,INT,p}$ from the raw radiometric data. Then $T_{B,EXT,p}$ were estimated using (2) for *Algorithm 1* and (4) and (5) for *Algorithm 2*. It should be noticed that $T_{B,p} = 0.5(T_{B,p,CH1} + T_{B,p,CH2})$.

A. JÜLBARA

The mean values of the data obtained between 13th and 26th April 2011, during the one hour sky measurements from 3 pm to 4 pm will be used to illustrate the radiometer behavior and the algorithm performance. The feed cable losses were measured in the High Frequency Laboratory, Peter Grünberg Institute, FZJ. The mean values for the frequency range 1.400 – 1.420 GHz were used, namely 0.15 dB and 0.133 dB for the feed cables for H-pol and V-pol, respectively.

Fig. 1(a) and Fig. 1(b) show the variations of the radiometer gain and the effective transmissivity $t_{eff,p}$ due to air temperature changes. It is obvious that both radiometer gain and effective transmissivity $t_{eff,p}$ depend on air temperature and decrease with increasing T_{air}.

The data obtained during continuous sky measurements from DOY 91.7132 to DOY 92.9715 were used to test the algorithm performance. Because of JÜLBARA orientation to the south, distinct contamination due to the sun emission was registered. The contaminated data from DOY 92.4396 to DOY 92.559 were removed and the remaining 1640 measurements were used for algorithm comparison. The results are summarized in Table 1.

In all tables $Delta = mean(T_{B,EXT,P}) - mean(T_{B,MODEL})$ is calculated for the corresponding data set.

TABLE 1
JÜLBARA RESULTS FROM DOY 91.71 TO DOY 92.97, N = 1640, $T_{B,MODEL}$ = 5.11 K

	Algorithm 1		*Algorithm 2*			
	Cable loss corr.		**Mean $t_{eff,p}$**		$t_{eff,p}$	
	$T_{B,H}$	$T_{B,V}$	$T_{B,H}$	$T_{B,V}$	$T_{B,H}$	$T_{B,V}$
Min	4.06	7.27	1.78	1.98	5.07	5.07
Max	12.39	15.34	10.20	10.25	5.13	5.13
Mean	**7.40**	**10.42**	**5.11**	**5.11**	**5.11**	**5.11**
std	1.16	1.13	1.16	1.13	0.02	0.02
Delta	**2.29**	**5.31**	**0.00**	**0.00**	**0.00**	**0.00**

From the results presented in Table 1 the following conclusions could be drawn: for *Algorithm 1* there is a systematic bias between $T_{B,EXT}$ and $T_{B,MODEL}$, namely 2.29 K and 5.31 K at H-pol and V-pol respectively; for *Algorithm 2* there is no bias. When *Algorithm 2* is used with the mean values of the effective transmissivities calculated for the whole data set (n=1640), the standard deviation is the same as for *Algorithm 1*. For *Algorithm 2* with the instantaneous values of $t_{eff,p}$, the standard deviation is very small.

Linear regression equations $t_{eff,H}$ (T_{air}) and $t_{eff,V}$ (T_{air}) were derived using the data set described above with n = 1640. Then *Algorithm 2* was tested with another independent data set collected from DOY 80.6684 to DOY 80.9178, total duration six hours and n = 359. The results are presented in Table 2. The linear regression equations $t_{eff,H}$ (T_{air}) and $t_{eff,V}$ (T_{air}) were used for estimating the effective transmissivities $t_{eff,p}$ from the measured air temperature T_{air}.

TABLE 2
JÜLBARA RESULTS FROM DOY 80.67 TO DOY 80.92, N = 359, $T_{B,MODEL}$ = 5.12 K

	Algorithm 1		*Algorithm 2*	
	Cable loss correction		**Linear regression $t_{eff,p}$ (T_{air})**	
	$T_{B,H}$	$T_{B,V}$	$T_{B,H}$	$T_{B,V}$
Min	3.76	6.35	2.98	2.53
Max	8.78	12.89	7.40	8.16
Mean	**6.81**	**9.64**	**5.43**	**5.23**
std	0.98	1.07	0.79	0.86
Delta	**1.69**	**4.52**	**0.31**	**0.11**

The comparison of the results estimated with *Algorithm 1* and *Algorithm 2* presented in Table 2 clearly shows the significant improvement of the calibration accuracy obtained using the new calibration algorithm – the bias is substantially

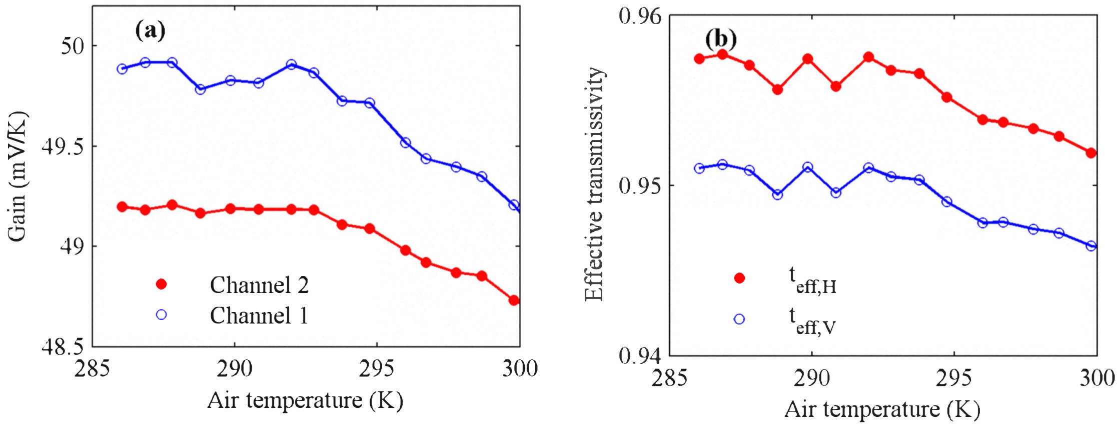

Fig. 1 (a) JÜLBARA gain variations with air temperature. (b) JÜLBARA effective transmissivity variations with air temperature.

reduced and the standard deviation is smaller.

B. ELBARA II

Distinct RFI were present in the sky radiometric data – bursts of the order of 40 to 60 K with a maximum of 450 K at H-polarization for DOY 207.378. The RFI-distorted periods were removed by using the following selection criterion:

$$abs((T_{B,CH1} - T_{B,CH2}) - mean(T_{B,CH1} - T_{B,CH2})) < 0.3K, \quad (6)$$

where $mean(T_{B,CH1} - T_{B,CH2})$ is the mean value calculated for the whole data set. The selection criterion given in (6) was applied for H-pol and V-pol data. Only the data fulfilling the criterion (6) simultaneously for H-pol and V-pol were used for algorithm testing. After the RFI removal, data set with n = 13489 was obtained.

The ELBARA II feed cable losses were specified as $L_H = L_V = 0.254$ dB by the manufacturer.

According to [2], the ELBARA II calibration assembly (CA) is designed as a separate module to allow for independent operation for cross calibration among other L-band radiometers. The temperature of the CA is stabilized to ± 0.1 K. The brightness temperature of the active cold source T_{ACS} was estimated from the measured temperature of the resistive noise source T_{RS}, mounted in the CA, using the linear regression equation given in [2, Section 3.1.4]. The brightness temperature T_{ACS} was calculated for every measurement cycle. Mean (T_{ACS}) = 40.99 K with standard deviation 0.016 K was obtained for the whole data set (n=13489). The corresponding values for the CA temperatures, namely mean (T_{RS})= 313.14 K and standard deviation 0.07 K confirmed the excellent temperature stability of the calibration assembly of ELBARA II reported in [3].

The two algorithms for estimating $T_{B,EXT,p}$ were applied and the results are presented in Table 3.

For *Algorithm 1* there is again a bias, namely – 1.76 K and – 0.42 K at H-pol and V-pol, respectively. The conclusions for *Algorithm 2* are similar to that for JÜLBARA – no bias and very small standard deviation, in case that the instantaneous values of $t_{eff,p}$ were used.

TABLE 3
ELBARA II RESULTS FROM DOY 192.68 TO DOY 223.99,
N = 13489, $T_{B,MODEL}$ = 4.92 K

	Algorithm 1		***Algorithm 2***			
	Cable loss corr.		**Mean $t_{eff,p}$**		**$t_{eff,p}$**	
	$T_{B,H}$	$T_{B,V}$	$T_{B,H}$	$T_{B,V}$	$T_{B,H}$	$T_{B,V}$
Min	1.99	3.09	3.79	3.50	4.88	4.88
Max	6.28	9.75	8.04	10.15	4.95	4.95
Mean	**3.16**	**4.50**	**4.92**	**4.92**	**4.92**	**4.92**
std	0.49	0.69	0.49	0.69	0.01	0.01
Delta	**- 1.76**	**- 0.42**	**0.00**	**0.00**	**0.00**	**0.00**

Fig. 2(a) and Fig. 2(b) show the dependence of effective transmissivities $t_{eff,H}$ and $t_{eff,V}$ on the air temperature. There are two clusters: the first cluster (top) contains data suggesting linear dependence of $t_{eff,H}$ and $t_{eff,V}$ vs. T_{air} (small gradients $\Delta t_{eff,p}/\Delta T_{air}$); the second cluster contains data that deviate slightly from this linear dependence and also relatively small numbers of outliers. From the histograms of $t_{eff,H}$ and $t_{eff,V}$ presented in Fig. 2(c) and Fig. 2(d) it can be seen that most of the data are close to the corresponding average values. At H-pol about 80% of the $t_{eff,H}$ data are in the range from 0.947 to 0.951, i.e. mean ($t_{eff,H}$) ± 0.002. At V-pol about 70% of the $t_{eff,V}$ data are in the range from 0.943 to 0.947, i.e. mean ($t_{eff,V}$) ± 0.002. It should be noticed that change of Δt_{eff} = 0.002 of the effective transmissivities $t_{eff,H}$ and $t_{eff,V}$ leads to a corresponding change of $\Delta T_{B,EXT,p} \approx \Delta t T_{air} \approx 0.6$ K. It should be also mentioned that the change of Δt_{eff} = 0.002 corresponds to cable loss change of ΔL = 0.01 dB.

From the results presented for JÜLBARA and ELBARA II radiometers, it is obvious that the effective transmissivities $t_{eff,H}$ and $t_{eff,V}$ estimated using (4) account for the feed cable loss effects and for the variations of the radiometer gain due to air temperature changes. The effective transmissivities also account for the effects of antenna loss. As shown in [5], the

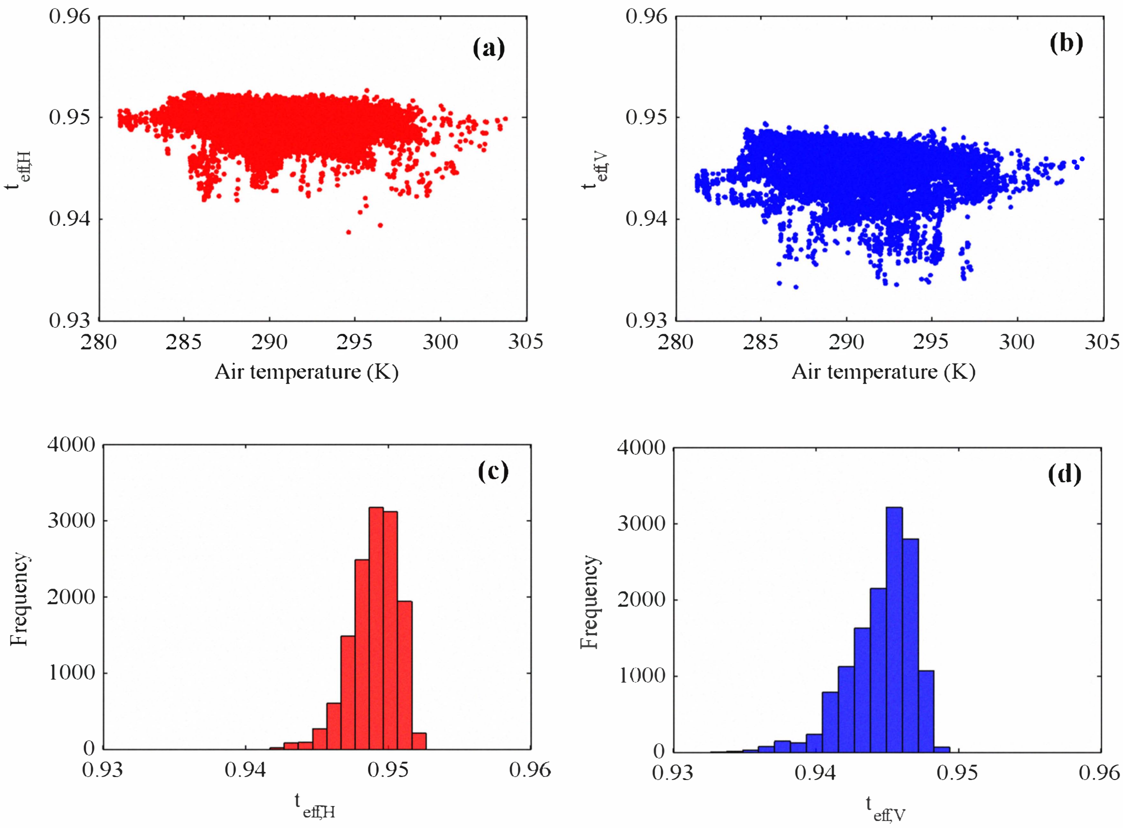

Fig. 2 ELBARA II effective transmissivities variations with air temperature: (a) horizontal polarization and (b) vertical polarization. Histograms of the effective transmissivities: (c) horizontal polarization and (d) vertical polarization.

antenna transmissivities for pyramidal rectangular horns are ≤ 1, namely 0.9920, 0.9872, and 0.9972 at 0.6, 0.82, and 2.5 GHz, respectively.

V. CONCLUSION

From this study the following conclusions could be drawn. The measured radiometric sky data must be RFI free. The air temperature may be used as a proxy for feed cable physical temperature, but care must be taken to ensure that the temperature sensor and the feed cables are protected from direct sunlight. The feed cable loss must be estimated very accurately in order to reduce the systematic bias of brightness temperatures obtained with *Algorithm 1*. It was shown that for JÜLBARA the effective transmissivities depend strongly on air temperature and decrease with increasing air temperature. It was proved that the linear regression equations $t_{eff,H}$ (T_{air}) and $t_{eff,V}$ (T_{air}) could be used for estimating the effective transmissivities from the measured air temperature. It was also shown that the new calibration algorithm reduces significantly the bias of brightness temperature estimates for both radiometers, especially for JÜLBARA.

We think that testing of the new calibration algorithm using data obtained with the other ELBARA II radiometers, currently operating in SMOS-relevant field campaigns in Europe, will be very beneficial for the radiometric community.

ACKNOWLEDGMENT

The authors express their thanks to H. Jagdfeld, T. Ortmanns and W. Schmitz from the Central Institute of Technology, FZJ. Special thanks to R. Harms and F. Engels from the Agrosphere Institute (IBG-3), to H. Meier from the Central Institute of Electronics, FZJ, and to A. Fox from the High Frequency Laboratory, Peter Grünberg Institute, FZJ.

The work presented here was carried out in the frame of the research group MUSIS funded by German Research Foundation (DFG) and of TERENO, funded by the Federal Ministry of Education and Research, Germany (BMBF).

REFERENCES

[1] Mätzler et al., “ELBARA, the ETH L-band Radiometer for soil-moisture research,” in *Proc. IEEE IGARSS*, 2003, vol. 5, pp. 3058–3060.

[2] M. Schwank et al., “ELBARA II, an L-band radiometer system for soil moisture research,” *Sens. MDPI*, vol. 10, no. 1, pp. 584–612, 2010.

[3] M. Schwank et al., “L-band properties of vine vegetation at the MELBEX III SMOS Cal/Val Site,” in press.

[4] T. Pellarin et al., “Two-year global simulation of L-band brightness temperatures over land,” *IEEE Trans. Geosci. Remote Sens.*, vol. 41, no. 9, pp. 2135–2139, Sep. 2003.

[5] M. Zannoni et al., “TRIS. I. Absolute measurements of the sky brightness temperature at 0.6, 0.82, and 2.5 GHz,” *The Astrophysical J.*, vol. 688, 12-23, Nov. 2008.